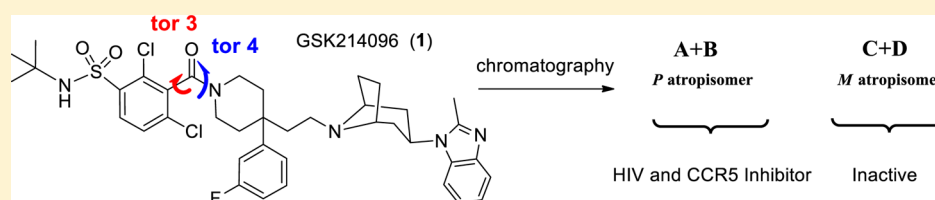


Biological and Structural Characterization of Rotamers of C–C Chemokine Receptor Type 5 (CCR5) Inhibitor GSK214096

Wieslaw M. Kazmierski,^{*,†} Susan Danehower,[†] Maosheng Duan,[†] Robert G. Ferris,[†] Vassil Elitzin,[‡] Douglas Minick,[‡] Matthew Sharp,[‡] Eugene Stewart,[‡] and Manon Villeneuve[‡][†]Infectious Diseases TAU and [‡]Platform Technology and Science, GlaxoSmithKline, Five Moore Drive, Research Triangle Park, North Carolina 27709-3398, United States

Supporting Information



ABSTRACT: We recently reported the discovery of preclinical CCR5 inhibitor GSK214096, **1** (*J. Med. Chem.* **2011**, *54*, 756). Detailed characterization of **1** revealed that it exists as a mixture of four separable atropisomers A–D. The two slow-interconverting pairs of rotamers A + B and C + D were separated and further characterized. HIV and CCR5-mediated chemotaxis data strongly suggest that the antiviral potency of **1** is due to rotamers A + B and not C + D. Furthermore, integrated UV, vibrational circular dichroism VCD and computational approach allowed to determine the *M* chirality in C + D (and *P* chirality in A + B). These findings imply additional avenues to be pursued toward new CCR5 antagonists.

KEYWORDS: CCR5, atropisomer, chemokine, antagonist, GSK214096, HIV inhibitor, entry inhibitor

A recent UNAIDS estimate puts the number of AIDS-related deaths at about 34 million worldwide since first cases were reported in 1981. Introduction of the Highly Active Antiretroviral Therapy (HAART) about two decades ago contributed to a dramatic decline in AIDS-related deaths in the developed world; nonetheless, there is a continued need for new approaches to the disease treatment and prevention. We recently reported the discovery of HIV-1 entry inhibitors GSK214096, **1**, and its clinical analogue GSK163929, **2** (Figure 1).^{1,2} In the initial HIV-

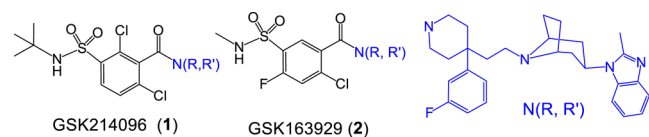


Figure 1. CCR5 antagonists **1** and **2**.

1 cell-entry step, the R5 HIV-1 glycoprotein 120 (gp120) binds to the CD4+ T-cell receptor. The resulting conformational change in gp120 facilitates its binding to the cellular coreceptor CCR5 (C–C chemokine receptor type 5). Compounds **1** and **2** bind CCR5 and thus inhibit CCR5-gp120 interaction, blocking subsequent HIV-1 entry steps and preventing the virus from infecting the immune cells.³ CCR5 is one of 19 chemokine receptors, which are known to be involved in regulating the immune response, sepsis, chronic obstructive pulmonary disease, asthma, inflammatory bowel disease, and cancer.^{4–6} A 32-base pair deletion mutation in the CCR5 gene has been associated with increased resistance to HIV-1 infection and with a slower

disease progression, providing strong rationale for targeting CCR5 for HIV therapy. Maraviroc is the only FDA-approved CCR5 antagonist, indicated for treatment of HIV infections.⁷ The CCR5 delta32 genotype has also been shown to be involved in the rheumatoid arthritis, allograft rejection, and liver protection against toxic injury, suggesting additional uses of CCR5 antagonists.^{8–13} CCR5 expression on the cell surface is regulated by its endogenous ligands; CCL3 (MIP-1 α), Macrophage Inflammatory Protein type 1 α), CCL4 (MIP-1 β), and CCL5 (RANTES, Regulated on Activation, Normal T Expressed and Secreted).^{14,15}

During the preclinical investigations it was found that the CCR5 antagonist **1** separates into two peaks on the achiral C₁₈ reverse phase column and into four peaks A–D on the Chiralpak AS-H column using SFC. Under these conditions compound **2** elutes as a single peak. Identical isotopic masses of A–D suggested that these compounds were atropisomers.

Drug development strategy for atropisomers and their classification into classes 1, 2, and 3 depend on their conversion kinetics.^{16,17} A mixture of rapidly converting atropisomers (class 1) of endothelin receptor antagonist BMS-207940 has been progressed to the clinic.¹⁸ A kilogram scale crystallization of key rotamer 4 out of the mixture of four stable atropisomers (class 3) of neurokinin antagonist ZM374979 has been reported.¹⁹ To further assess the suitability of **1** or A–D for development, we

Received: September 1, 2014

Accepted: October 28, 2014

Published: October 28, 2014

preparatively isolated all four rotamers A–D as well as pairs A + B and C + D (Figure 2). Rotamers A and D, as well as B and C,

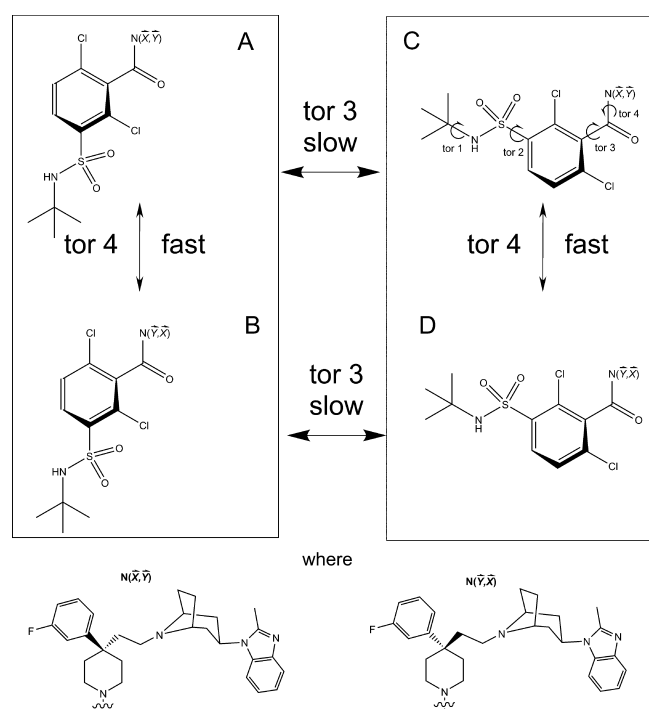


Figure 2. Atropisomers of **1**, A–D (assignments arbitrary). Assignment of torsions (tor) 3 and 4 is discussed in the text.

are enantiomeric pairs. Rotamers A and C, as well as B and D, are diastereomeric pairs. The atropisomer interconversion half-lives were determined by quantitating peaks corresponding to A–D and arising from either A or A + B (Table 1).²⁰ The A ↔ B (and

Table 1. Rotamer Interconversion Kinetics

temp (°C)	A ↔ B (C ↔ D) ^a	<i>t</i> _{1/2} (days)
5.4		2.083
26.8		0.113
37.8		0.025
	A + B ↔ C + D ^b	
25		161 ^c
37		37 ^c
43		22
60		1.8
73		1

^aAchiral Bonus-RP HPLC column; sample concentration 0.75 mg/mL in 60:40 water/acetonitrile. ^bChiralpak AS-H chiral SFC column; sample concentration 2 mg/mL in ethanol. ^cCalculated according to ref 20.

by symmetry C ↔ D) conversion was found to be relatively fast (*t*_{1/2} = 0.6 h, 0.025 day), while the A + B ↔ C + D conversion was much slower (*t*_{1/2} ≈ 888 h, 37 days) in solution at 37.8 °C (Table 1).²⁰ Both A + B and C + D were stable as solids over several months at room temperature (data not shown).

We characterized A + B and C + D by the IR and vibrational circular dichroism (VCD).^{21–23} As anticipated for enantiomers, the VCD and IR spectra for C + D were, respectively, a mirror image and identical compared to the spectra of A + B (not shown) (Figure 3). We then utilized the VCD to determine the

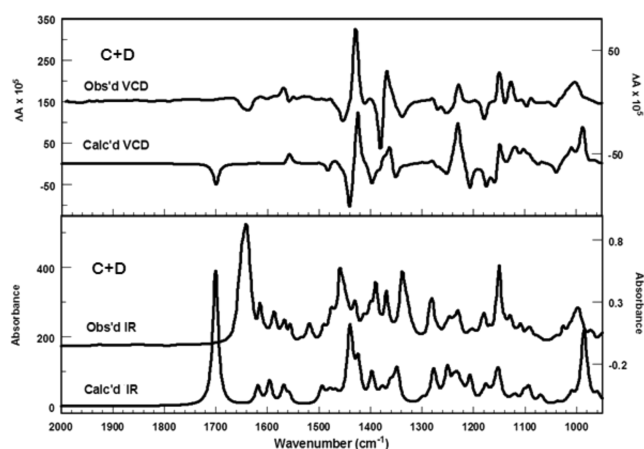


Figure 3. Observed IR and VCD spectra of C + D and calculated spectra for reduced structure model (M)-3 (Figure 4).

absolute configuration of A + B and C + D. In order to calculate the VCD spectra for the appropriate model structure, we first had to identify the two highest rotational barriers giving rise to four atropisomers. As torsions 1 and 2 as well as 3 and 4 are coupled (Figure 2), a full torsional profile was determined around these bonds using ab initio calculations at the RHF/6-31G** level.²⁴ Calculations of relative barriers to rotation revealed that torsion 3 (24.4 kcal/mol) and torsion 4 (18.4 kcal/mol) had the highest rotational barriers. In contrast, torsion 1 (10.5 kcal/mol) and torsion 2 (5.7 kcal/mol) had much lower rotational barriers. Thus, atropisomers A–D formed by a relatively slow rotation around torsion 3 and a fast rotation around torsion 4. For both torsions 3 and 4, rotational barriers and half-lives at 37.8 °C indicated class 2 atropisomers.^{16,17} Next, theoretical VCD spectra were calculated for one of the configurational possibilities around the prominent torsion 3. Since flexibility of the N(R,R') moiety in **1** would require computations of a large number of conformational models (overall contribution of which would be minor due to conformational averaging), further computations were performed on the reduced structure atropisomer (M)-3 (Figure 4). Comparison of the VCD and IR spectra calculated for

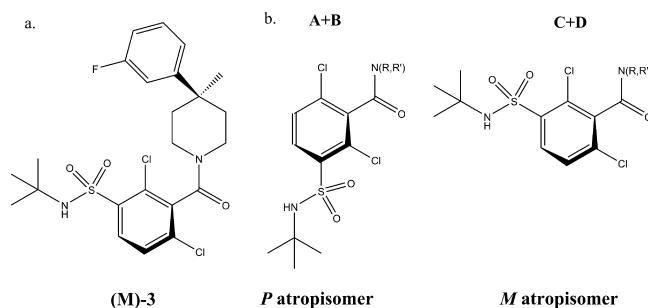


Figure 4. (a) Reduced structure model amide atropisomer (M)-3 used for theoretical VCD calculations. (b) Axial chirality assignments for A + B and C + D. N(R,R') as in Figure 1

(M)-3 were found to be in excellent agreement with the experimental VCD and IR spectra for C + D and indicated the M axial chirality at >99% confidence level (Figure 4).

Stability of A + B and C + D as solids and long interconversion half-life *t*_{1/2} = 37 days in solution at 37 °C allowed determination of their inhibitory potencies in the HIV-1 as well as ligand-stimulated chemotaxis inhibition assays (Table 2).

Table 2. HIV-1 and Chemotaxis Inhibition

	IC ₅₀ (nM) Ba-L		inhibition of ligand-stimulated chemotaxis in CEM cells, IC ₅₀ (nM)		
	HOS	PBL	RANTES	MIP-1 α	MIP-1 β
aplaviroc	1.6	2.1	2.5	3.3	1.8
vicriviroc	2.1	6.5	2.5	2.3	3.6
2	4.3	3.5	5.6	16.3	4.7
1	4.9	3.1	28.8	33.1	25.6
A + B	3.3	0.8	4.8	32.1	16.3
C + D	30	27.8	a	a	a
AMD3100	a	a	a	a	a

^aZero % inhibition at 2.0 μ M compound concentration. HOS and PBL cells infected with M-tropic Ba-L HIV were used to determine the antiviral properties of compounds. Chemotaxis assays; human CEM cells expressing both CCR5 and CXCR4 were challenged with EC₈₀ concentrations of RANTES (5 nM), MIP-1 α (10 nM), and MIP-1 β (10 nM). Each IC₅₀ is a mean of at least six independent experiments. All dilutions were prepared from solid A + B and C + D and used immediately.

As expected, the control CXCR4 antagonist AMD3100 was inactive in both the CCR5-mediated HIV and CCR5-chemotaxis assays. Aplaviroc, vicriviroc, **1**, **2**, and A + B were very potent in all assays. Rotamers C + D exhibited some (1/10–1/30th of A + B) inhibitory potency in cellular HOS and PBL antiviral assays. This is likely due to small amounts of A + B formed in situ from C + D during the course of these assays.²⁵ However, in the much faster chemotaxis assay, C + D was found to be completely inactive. These results indicate that A + B (but not C + D) interact with CCR5. The HIV and chemotaxis inhibitory potency of **1** is thus due to A + B, while C + D does not interact with CCR5 and does not contribute to activity. In yet another manifestation of the distinctly different properties of pairs A + B and C + D, the latter was found to have substantially lower in vivo clearance and greater systemic exposure from oral dosing relative to the former in both rat and dog PK (Table 3).

In summary, we determined that **1** is a mixture of four separable atropisomers A–D. Because of restricted rotation around torsion 3, pairs A + B and C + D were sufficiently stable to allow further characterization and were demonstrated to have distinct properties. The combined potency and structural data suggest that P(A + B) atropisomer, and not M(C + D), interacts with CCR5 and inhibits HIV and chemotaxis. This level of structural detail is unprecedented for CCR5 inhibitors and allows to further refine the CCR5 pharmacophore models.¹ Investigations of other advanced CCR5 antagonists^{26–28} suggested very fast atropisomer conversion rates for SCH351125²⁷ around both torsion 3 (max. $t_{1/2}$ = 30 h) and torsion 4 (max. $t_{1/2}$ = 5.6 h). Thus, the 2,6-dichloro motif in benzamide **1** increased the rotation half-life around torsion 3 more than 30-fold vs the 2,6-dimethyl benzamide motif in SCH351125. This also suggests that further structural modifications in either the 2,6-disubstituted aryl or alternatively in the adjacent-piperidine

ring may lead to conformationally stable (class 3) tertiary amide-based CCR5 antagonists.

■ ASSOCIATED CONTENT

Supporting Information

Description of viral and chemotaxis assays. ¹H NMR of A + B and C + D. Description of VCD experiments. Calculation of kinetic parameters. This material is available free of charge via the Internet at <http://pubs.acs.org>.

■ AUTHOR INFORMATION

Corresponding Author

*Tel: +9194839462. Fax: +9193156053. E-mail: wieslaw.m.kazmierski@gsk.com.

Author Contributions

The manuscript was written through contributions of all authors. All authors have given approval to the final version of the manuscript.

Notes

The authors declare no competing financial interest.

■ ACKNOWLEDGMENTS

We thank Drs. Peimin Shao and Pat Wheelan their skilful contributions to generating data in Tables 1 and 3.

■ DEDICATION

Dedicated to Professor Victor J. Hruby on the occasion of his 75th birthday.

■ ABBREVIATIONS

CCR2, CC chemokine receptor 2; CCL2, CC chemokine ligand 2; CCR5, CC chemokine receptor 5; VCD, vibrational circular dichroism; CCR5, CC chemokine receptor type 5; HOS, human osteosarcoma; PBL, peripheral blood lymphocytes; MIP-1 α , macrophage inflammatory protein type 1 α ; RANTES, regulated on activation, normal T expressed and secreted; HAART, highly active antiretroviral therapy; SFC, Supercritical Fluid Chromatography

■ REFERENCES

- (1) Kazmierski, W. M.; Aquino, C.; Chauder, B. A.; Deanda, F.; Ferris, R.; Jones-Hertzog, D. K.; Kenakin, T.; Koble, C. S.; Watson, C.; Wheelan, P.; Yang, H.; Youngman, M. Discovery of bioavailable 4,4-disubstituted piperidines as potent ligands of the chemokine receptor 5 and inhibitors of the human immunodeficiency virus-1. *J. Med. Chem.* **2008**, *51*, 6538–6546.
- (2) Kazmierski, W. M.; Anderson, D. L.; Aquino, C.; Chauder, B. A.; Duan, M.; Ferris, R.; Kenakin, T.; Koble, C. S.; Lang, D. G.; McIntyre, M. S.; Peckham, J.; Watson, C.; Wheelan, P.; Spaltenstein, A.; Wire, M. B.; Svolto, A.; Youngman, M. Novel 4,4-disubstituted piperidine-based C-C chemokine receptor-5 inhibitors with high potency against human immunodeficiency virus-1 and an improved human ether-a-go-go related gene (hERG) profile. *J. Med. Chem.* **2011**, *54*, 3756–3767.

Table 3. Rat and Dog PK of A + B and C + D^a

	rat			dog		
	Cl (mL/min/kg)	PO AUC (h-ng/mL)	%F	Cl (mL/min/kg)	PO AUC (h-ng/mL)	%F
A + B	14.3	234	19	9.8	407	23
C + D	7.9	413	19	3.0	1668	29

^aAll values are averages of $n = 3$ at 1 mg/kg iv and po doses. All doses were prepared from solid samples and used immediately. Both A + B and C + D were cross-monitored.

- (3) Tsubris, A. M. N.; Kuritzkes, D. R. Chemokine antagonists as therapeutics: Focus on HIV-1. *Annu. Rev. Med.* **2007**, *58*, 445–459.
- (4) Haskell, C. A.; Horuk, R. Lymphocyte Trafficking in Health and Disease. In *Progress in Inflammation Research*; Badolato, R., Sozzani, S., Eds.; Birkhäuser: Basel, Switzerland, 2006; pp 181–196.
- (5) Zlotnik, A. Chemokines and cancer. *Int. J. Cancer* **2006**, *119*, 2026–2029.
- (6) Wells, T. N. C.; Power, C. A.; Shaw, J. P.; Proudfoot, A. E. I. Chemokine blockers: Therapeutics in the making? *Trends Pharmacol. Sci.* **2006**, *27*, 41–47.
- (7) Dorr, P.; Westby, M.; Dobbs, D.; Griffin, P.; Irvine, B.; Macartney, M.; Mori, J.; Rickett, G.; Smith-Burchnell, C.; Napier, C.; Webster, R.; Armour, D.; Price, D.; Stammen, B.; Wood, A.; Perros, M. Maraviroc (UK-427,857), a potent, orally bioavailable, and selective small-molecule inhibitor of chemokine receptor CCR5 with broad-spectrum anti-human immunodeficiency virus type 1 activity. *Antimicrob. Agents Chemother.* **2005**, *49*, 4721–4732.
- (8) Gómez-Reino, J. J.; Pablos, J. L.; Carreira, P. E.; Santiago, B.; Serrano, L.; Vicario, J. L.; Balsa, A.; Figueroa, M.; De Juan, M. D. Association of rheumatoid arthritis with a functional chemokine receptor, CCR5. *Arthritis Rheum.* **1999**, *42*, 989–992.
- (9) Fildes, J. E.; Walker, A. H.; Howlet, R.; Bittar, M. N.; Hutchinson, I. V.; Leonard, C. T.; Yonaneimail, N. Donor CCR5 $\Delta 32$ polymorphism and outcome following cardiac transplantation. *Transplant. Proc.* **2005**, *37*, 2247.
- (10) Ajuebor, M. N.; Aspinall, A. I.; Zhou, F.; Le, T.; Yang, Y.; Urbanski, S. J.; Sidobre, S.; Kronenberg, M.; Hogaboam, C. M.; Swain, M. G. Lack of chemokine receptor CCR5 promotes murine fulminant liver failure by preventing the apoptosis of activated CD1d-restricted NKT cells. *J. Immunol.* **2005**, *174*, 8027–8037.
- (11) Ajuebor, M. N.; Carey, J. A.; Swain, M. G. CCR5 in T cell-mediated liver diseases: What's going on? *J. Immunol.* **2006**, *177*, 2039–2045.
- (12) Ajuebor, M. N.; Wondimu, Z.; Hogaboam, C. M.; Le, T.; Proudfoot, A. E. I.; Swain, M. G. CCR5 deficiency drives enhanced natural killer cell trafficking to and activation within the liver in Murine T cell-mediated hepatitis. *Am. J. Pathol.* **2007**, *170*, 1975–1988.
- (13) Moreno, C.; Gustot, T.; Nicaise, C.; Quertinmont, E.; Nagy, N.; Parmentier, M.; Le Moine, O.; Devière, J.; Louis, H. CCR5 deficiency exacerbates T-cell-mediated hepatitis in mice. *Hepatology* **2005**, *42*, 854–862.
- (14) Jones, K. L.; Maguire, J. J.; Davenport, A. P. Chemokine receptor CCR5: from AIDS to atherosclerosis. *Br. J. Pharmacol.* **2011**, *162*, 1453–1469.
- (15) Gonzalez, E.; Kulkarni, H.; Bolivar, H.; Mangano, A.; Sanchez, R.; Catano, G.; Nibbs, R. J.; Freedman, B. I.; Quinones, M. P.; Bamshad, M. J.; Murthy, K. K.; Rovin, B. H.; Bradley, W.; Clark, R. A.; Anderson, S. A.; O'Connell, R. J.; Agan, B. K.; Ahuja, S. S.; Bologna, R.; Sen, L.; Dolan, M. J.; Ahuja, S. K. The influence of CCL3L1 gene-containing segmental duplications on HIV-1/AIDS susceptibility. *Science* **2005**, *307*, 14334–11440.
- (16) LaPlante, S. R.; Edwards, P. J.; Fader, L. D.; Jakalian, A.; Hucke, O. Revealing atropisomer axial chirality in drug discovery. *ChemMedChem* **2011**, *6*, 505–513.
- (17) LaPlante, S. R.; Fader, L. D.; Fandrick, K. R.; Fandrick, D. R.; Hucke, O.; Kemper, R.; Miller, S. P. F.; Edwards, P. J. Assessing atropisomer axial chirality in drug discovery and development. *J. Med. Chem.* **2011**, *54*, 7005–7022.
- (18) Zhou, Y. S.; Tay, L. K.; Hughes, D.; Donahue, S. Simulation of the impact of atropisomer interconversion on plasma exposure of atropisomers of an endothelin receptor antagonist. *J. Clin. Pharmacol.* **2004**, *44*, 680–688.
- (19) Parker, J. S.; Smith, N. A.; Welham, M. J.; Moss, W. O. New approach to the rapid parallel development of four neurokinin antagonists. Part 5. Preparation of ZM374979 cyanoacid and selective crystallisation of ZM374979 atropisomers. *Org. Process. Res. Dev.* **2004**, *8*, 45–50.
- (20) Atwood, J. D. Integrated Rate Expressions. In *Inorganic and Organometallic Reaction Mechanisms*; Brooks/Cole Publishing: Monterey, CA, 1985; pp 3–17.
- (21) Freedman, T. B.; Cao, X.; Nafie, L. A.; Kalbermatter, M.; Linden, A.; Rippert, A. J. An unexpected atropisomerically stable 1,1-biphenyl at ambient temperature in solution, elucidated by vibrational circular dichroism (VCD). *Helv. Chim. Acta* **2003**, *86*, 3141–3155.
- (22) Stephens, P. J.; Devlin, F. J.; Pan, J.-J. The determination of the absolute configurations of chiral molecules using vibrational circular dichroism (VCD) spectroscopy. *Chirality* **2008**, *20*, 643–663.
- (23) Freedman, T. B.; Cao, X.; Dukor, R. K.; Nafie, L. A. Absolute configuration determination of chiral molecules in the solution state using vibrational circular dichroism. *Chirality* **2003**, *15*, 743–748.
- (24) Jalkanen, K. J.; Suhai, S. N-Acetyl-L-alanine N'-methylamide: a density functional analysis of the vibrational absorption and vibrational circular dichroism spectra. *Chem. Phys.* **1996**, *208*, 81–116.
- (25) Reversible first-order kinetics calculations (ref 21) reveal that, starting from pure C + D, 93:7 enantiomeric ratio of A + B/C + D will be reached after 4 days at 37 °C.
- (26) Thoma, G.; Nuninger, F.; Schaefer, M.; Akyel, K. G.; Albert, R.; Beerli, C.; Bruns, C.; Francotte, E.; Luyten, M.; MacKenzie, D.; Oberer, L.; Streiff, M. B.; Wagner, T.; Walter, H.; Weckbecker, G.; Zerwes, H.-G. Orally bioavailable competitive CCR5 antagonists. *J. Med. Chem.* **2004**, *47*, 1939–1955.
- (27) Palani, A.; Shapiro, S.; Clader, J. W.; Greenlee, W. J.; Blythin, D.; Cox, K.; Wagner, N. E.; Strizki, J.; Baroudy, B. M.; Dand, N. *Bioorg. Med. Chem. Lett.* **2003**, *13*, 705–708.
- (28) McCombie, S. W.; Tagat, J. R.; Vice, S. F.; Lin, S.-I.; Steensma, R.; Palani, A.; Neustadt, B. R.; Baroudy, B. M.; Strizki, J. M.; Endres, M.; Cox, K.; Dan, N.; Chou, C.-C. Piperazine-based CCR5 antagonists as HIV-1 inhibitors. III: Synthesis, antiviral and pharmacokinetic profiles of symmetrical heteroaryl carboxamides. *Bioorg. Med. Chem. Lett.* **2003**, *567*–571.